Vol 11 No 1, January 2002
1009-1963/2002/11(01)/0021-09

Chinese Physics

© 2002 Chin. Phys. Soc.
and IOP Publishing Ltd

Influence of intensity on the steady and transient state space-charge fields in photorefractive polymers*

Yuan Bao-Hong(袁保红), Sun Xiu-Dong(孙秀冬), Jiang Yong-Yuan(姜永远),
Zhou Zhong-Xiang(周忠祥), Yao Feng-Feng(姚凤凤), and Li Yan(李 焱)
Department of Applied Physics, Harbin Institute of Technology, Harbin 150001, *China*

(Received 8 March 2001; revised manuscript received 28 August 2001)

We have proven theoretically that there are sublinear, linear and superlinear relations between the response rates and total incident intensity for different cases of traps in photorefractive polymer materials. These relations were observed in inorganic photorefractive crystals many years ago. Also, the steady-state space-charge field is a function of the total incident intensity, which has also been found in inorganic photorefractive crystals. We have measured the relations of the steady-state diffraction efficiency and the response rate with respect to the total incident intensity in the photorefractive composite consisting of the polymer (N-vinylcarbazole) (PVK) doped with 4,4'-n-pentylcyanobiphenyl (5CB) and C_{60}. The results obtained show that the composite belongs to the case of low trap density.

Keywords: photorefractive polymer, space-charge field, response rate
PACC: 4240, 4270G

1. Introduction

During the past decades, the photorefractive (PR) effect has been extensively investigated and applied to various fields, such as image storage, optics information processing, and amplification of optics signal, etc.[1−8] Especially, since Ducharme[9] first observed the PR effect in the polymer of bisA-NPDA:DEH in 1991, polymers have become very popular PR materials. Until now, materials and theories of photorefractive polymers (PRPs) have been highly developed.[10−14]

The following three anomalous phenomena, which cannot be explained by the "standard band transport model", have attracted the attention of many researcher: the bi-exponential or tri-exponential form of the formation of the space-charge field (SCF) in inorganic PR crystals; the nonlinear relation between response rates of the SCF and the total incident intensity; and the dependence of the steady-state SCF (including amplitude and phase) on the total incident intensity. For inorganic PR crystals, these three problems were found in experiments and explained by many models, such as the two species of carriers (electron and hole) with multiple traps (shallow and deep traps).[15−20] For PRPs, the three subjects are just being researched. In fact, many researchers have reported a bi-exponential form of the SCF during the formation and erasure processes in PRP materials.[21−25] We have theoretically explained this bi-exponential form of the SCF and discussed the effect of an applied electric field on the SCF.[26,27] However, the second and the third subjects mentioned above have not been studied for PRPs until now. In this paper, we discuss the dependence of the steady-state SCF and the response rates on the incident intensity.

2. Model equations

According to Refs.[26] and [27], we know that the dynamic equation of the first-order Fourier component of the SCF can be written as

$$\ddot{E}_1 + \gamma \dot{E}_1 + \omega_0^2 E_1 = f, \tag{1}$$

where

$$\begin{aligned}
\gamma =& \gamma' + \mathrm{i}k, \\
\omega_0^2 =& \omega_\mathrm{R}^2 + \mathrm{i}\omega_\mathrm{I}^2 \\
f =& \left[- r_1(T_\mathrm{i} - T_0) + T_1 \left(r_0 - \frac{g}{N_\mathrm{i}} \right) \right. \\
& \left. + \frac{g}{N_\mathrm{i}} m(\rho_0 + T_\mathrm{i} - T_0 - N_\mathrm{i}) \right],
\end{aligned}$$

*Project supported by the National Natural Science Foundation of China (Grant No. 69878006), and the Foundation of Harbin Institute of Technology, China (Grant No. 991190-014).

and

$$\gamma' = \frac{g}{N_{\rm i}} + T_{\rm i} + \rho_0\left(\frac{1}{2}c + 3\right) + \xi k^2,$$

$$\begin{aligned}\omega_{\rm R}^2 =& \rho_0\left(\frac{1}{2}c + 1\right)\left(\frac{g}{N_{\rm i}} + 2\rho_0 + T_{\rm i}\right)\\ &- \left(\frac{1}{2}c\rho_0(\rho_0 + T_{\rm i} - T_0)\right.\\ &\left.+ \frac{g}{N_{\rm i}}P(\rho_0 + T_{\rm i} - T_0 - N_{\rm i}) + \frac{1}{2}c\rho_0 T_0\right),\end{aligned}$$

$$\omega_{\rm I}^2 = k\left(\frac{g}{N_{\rm i}} + \rho_0\right),$$

$$\begin{aligned}T_0 =& \frac{r_0 T_{\rm i}}{\rho_0 + r_0},\\ T_1 =& \frac{r_1(T_{\rm i} - T_0)}{\rho_0 + r_0}\left[1 - \exp[-(\rho_0 + r_0)t]\right],\\ r_0 =& \tau(s_{\rm T} I_0 + \beta'), \quad r_1 = s_{\rm T} I_0 m\tau,\\ g =& \frac{\alpha'\Phi_{\rm i} I_0\tau}{h\nu\sigma}, \quad \xi = \frac{k_{\rm B}T'}{eE_{\rm i}L},\end{aligned}$$

$$\rho_0 = \frac{g[1 - (T_{\rm i} - T_0)/N_{\rm i}] + r_0(T_{\rm i} - T_0)}{(g/N_{\rm i}) + (\rho_0 + T_{\rm i} - T_0) + T_0}.$$

Here ρ_0 is the zero-order Fourier component of the hole density; $N_{\rm i}$ is the total acceptor density; $T_{\rm i}$ is the total trap density; T_0 and T_1 are the zero-order and the first-order Fourier components of the empty trap density, respectively; r_0 and r_1 are the zero-order and the first-order Fourier components of the untrapping rate, respectively; g is the hole density generated per unit of time at the total acceptor concentration $N_{\rm i}$ and the applied electric field E_0 at the total intensity $I_{\rm i}$ ($g = \dfrac{\alpha'\Phi_{\rm i} I_{\rm i}\tau}{h\nu\sigma}$, where $\Phi_{\rm i}$ is the initial charge generation quantum efficiency when the SCF does not exist, $I_{\rm i}$ is the total incident intensity of the two incident beams, α' is the absorption index of the polymer, τ and σ are the units of time and density, and $h\nu$ is the energy of photons); k is the grating wave vector; m is the modulation of intensity; P and c are constants determined by experiment about the electric field dependence of the photocharge generation quantum efficiency and carrier mobility; $k_{\rm B}$ is Boltzmann's constant; T' is absolute temperature; $s_{\rm T}$ is the light excitation cross section of traps; and β' is the thermal excitation rate of traps. All the quantities are presented in a dimensionless form, and have been discussed in detail in Refs.[26]–[30].

In fact, Eq.(1) is a forced oscillation equation with damping. γ is the complex damping coefficient and ω_0 is the complex eigenfrequency of the PRP materials. f is the external driving force which is dependent on the intensity distribution I. This means that the formation of the SCF in PRPs is a forced vibration process with resistance. If the time dependence of T_1 is neglected, f is a constant when the intensity distribution I is of a stationary interference pattern; f gains the same form as I when I is of a moving or vibrational interference pattern. So we can regard I as an external driving force.

As mentioned above, when T_1 or the time dependence of T_1 can be neglected, f becomes a constant and we denote it as f_0. Using the two conditions given in Ref.[26], which are $E_1|_{t=0} = 0$ and $\dot{E}_1|_{t=0} = 0$, we rewrite the solution of Eq.(1) as follows

$$\begin{aligned}E_1 =& E_{\rm sc}^{\rm ss}\left[1 - \left(\frac{c_2}{c_2 - c_1}\right)\exp(c_1 t)\right.\\ &\left. - \left(1 - \frac{c_2}{c_2 - c_1}\right)\exp(c_2 t)\right],\end{aligned} \tag{2}$$

where $E_{\rm sc}^{\rm ss} = \dfrac{f_0}{\omega_0^2}$, which is a steady-state SCF. Then $c_{1,2} = \dfrac{-\gamma \mp \sqrt{\gamma^2 - 4\omega_0^2}}{2}$, which are complex. Equation (2) implies that there are two response rates during the formation of the SCF.

When the time dependence T_1 cannot be neglected, we rewrite f as

$$f = f_0 + f_1\exp(c_{\rm T} t), \tag{3}$$

where f_0 is the constant part of f and f_1 is the amplitude of variable part of f. $c_{\rm T}$ is the decay constant of traps, which equals $-(\rho_0 + r_0)$ and is real. Finally, we obtain the solution of Eq.(1)

$$\begin{aligned}E_1 =& E_{\rm sc}^{\rm ss}\left[1 - \left(\frac{c_2}{c_2 - c_1}\right)\left(1 - \Delta_1\frac{f_1}{f_0}\right)\exp(c_1 t)\right.\\ &- \left(1 - \frac{c_2}{c_2 - c_1}\right)\left(1 - \Delta_2\frac{f_1}{f_0}\right)\\ &\left.\times\exp(c_2 t) - \Delta_1\Delta_2\left(-\frac{f_1}{f_0}\right)\exp(c_{\rm T} t)\right],\end{aligned} \tag{4}$$

where $\Delta_1 = c_1/(c_{\rm T} - c_1)$ and $\Delta_2 = c_2/(c_{\rm T} - c_2)$. Now, we have three response rates ($-{\rm Re}(c_1)$, $-{\rm Re}(c_2)$ and $-c_{\rm T}$) for the formation of the SCF. Obviously the first two on the right-hand side of Eq.(4) describe the properties of the formation of SCF, and the last represents the characteristics of trapping and detrapping. Now it is necessary to note that all the results can be applied to the inorganic crystals only if $c = 0$, $P = 0$, and $T_{\rm i}$ is a large constant. The initial trap density $T_{\rm i}$ and the initial acceptor density $N_{\rm i}$, which are used in polymers, correspond to the quantities $N_{\rm A}$ and $N_{\rm D}$ used in inorganic PR crystals, respectively.

3. Discussion

3.1. Cases where f is a constant

In Ref.[22], the real form of the SCF was written as

$$\begin{aligned} E(x,t) =& E_0 + \frac{E_1}{2}\exp(\mathrm{i}kx) + \frac{E_1^*}{2}\exp(-\mathrm{i}kx) \\ =& E_0 + R_1[\cos(kx+\Phi_1) - R_2 \\ & \times \exp(-t/\tau_{\mathrm{sc}\ 1})\cos(kx+\Omega_1 t+\Phi_1+\Phi_2) - R_3 \\ & \times \exp(-t/\tau_{\mathrm{sc}\ 2})\cos(kx+\Omega_2 t+\Phi_1+\Phi_3)]. \end{aligned} \tag{5}$$

Here, R_1 and Φ_1 are the amplitude and the phase of the steady-state SCF $E_{\mathrm{sc}}^{\mathrm{ss}}$, respectively; R_2 and Φ_2 are the amplitude and the phase of $\left[\dfrac{c_2}{c_2-c_1}\right]$; R_3 and Φ_3 are the amplitude and the phase of $\left[1-\dfrac{c_2}{c_2-c_1}\right]$.

According to Ref.[27], we know that the amplitude and the phase of the steady-state SCF can be expressed as

$$R_1 = \frac{|f_0|}{[(\omega_{\mathrm{R}}^2)^2 + (\omega_{\mathrm{I}}^2)^2]^{1/2}}, \tag{6}$$

$$\Phi_1 = \pi - \text{arc tan}\frac{\omega_{\mathrm{I}}^2}{\omega_{\mathrm{R}}^2} \quad (\text{for the case of } \omega_{\mathrm{R}}^2 > 0),$$

or

$$\Phi_1 = -\text{arc tan}\frac{\omega_{\mathrm{I}}^2}{\omega_{\mathrm{R}}^2} \quad (\text{for the case of } \omega_{\mathrm{R}}^2 < 0), \tag{7}$$

$$\frac{-1}{\tau_{\mathrm{sc}\ 1,2}} = \mathrm{Re}(c_{1,2}) = \left[\frac{-\sqrt{2}\gamma' \mp (\sqrt{\alpha^2+\beta^2}+\alpha)^{1/2}}{2\sqrt{2}}\right], \tag{8}$$

where

$$\alpha = \gamma'^2 - k^2 - 4\omega_{\mathrm{R}}^2, \quad \beta = 2\gamma' k - 4\omega_{\mathrm{I}}^2.$$

Except for the total intensity of the two incident beams I_{i} and the grating wave vector k, which are variables in this paper, other parameters are set to the same values as those described in Refs.[29] and [30].

(1) If L=100μm, E_{i}=100V/μm, μ_{i}=10^{-7}cm^2/Vs and ε_{r}=3.5, we have σ=1.9×10^{20}/m^3 and τ=0.1s.

(2) N_{i}=7.6×10^4 (in units of σ).

(3) P=1 and c=2.8.

(4) The index of absorption of the polymer α'=10cm^{-1}; wavelength λ=0.7μm; the initial charge generation quantum efficiency Φ_{i}=0.01. Thereby we have

$$g = \frac{\alpha' \Phi_{\mathrm{i}} I_{\mathrm{i}} \tau}{h\nu\sigma} = 180 I_{\mathrm{i}}. \tag{9}$$

(5) From temperature T'=293K and the modulation of intensity m=1, we obtain ξ=2.527×10^{-6}.

(6) s_{T}=2cm^2/J and β'=0.02s^{-1}.

3.1.1. Case without traps

When no traps are present, it follows that $\gamma_{\mathrm{R0}} = \gamma_{\mathrm{R1}} = 0$, $r_0 = r_1 = 0$, and $T_0 = T_1 = T_{\mathrm{i}} = 0$. Therefore we can obtain $\rho_0 \approx \sqrt{g}$, $\gamma' \approx 4.4\sqrt{g}$, $\omega_{\mathrm{R}}^2 \approx 4.4g, \omega_{\mathrm{I}}^2 \approx k\sqrt{g}$, $f_0 \approx -gm$, $f_1 = 0$. Figure 1 plots the relations between R_1, Φ_1, $\tau_{\mathrm{sc}\ 1,2}^{-1}$, and the total intensity I_{i}. This implies that the amplitude of the steady-state SCF is enhanced with the increase of I_{i}, while the phase deviates from 90°. In fact, similar results have been found in inorganic PR crystals[15] in which this was attributed to the existence of shallow traps. But, in this paper, we directly attain it from the basic equations. Figure 1(c) shows $\tau_{\mathrm{sc}\ 1,2}^{-1} \propto I_{\mathrm{i}}^{1/2}$ for the case without traps, which agrees with the relation between the erasure rate and the intensity I_{i} in Ref.[21]. Usually, the formation of the photorefractive SCF refers to the trapping of the free carriers in inorganic crystals. However, the SCF is still induced by the free carriers, which drift to the dark areas, and the ionized acceptor centres in bright areas of polymers for the case without traps, although the free carriers in the dark area are not trapped. Hence, we believe that the SCF in the case without traps is unstable and its magnitude is directly related to the density of the free carriers that are dependent on the total intensity I_{i}. If one of the recording beams is cut off, the free carriers will quickly diffuse and approach a uniform distribution so that the SCF easily disappears. Also, comparing Fig.1(a) with the following Figs.4(a) and 4(c), we know that the magnitude of the SCF in the case without traps is much smaller than that in the case with traps.

3.1.2. Case with deep traps

For deep traps, which do not have high-density, we assume that, before the formation of the SCF, mainly the photo-induced carriers are trapped because the detrapping rate is always zero. So, during the formation of the SCF, we have $\gamma_{\mathrm{R0}} \neq 0$, $\gamma_{\mathrm{R1}} \neq 0$, $r_0 = r_1 = 0$, $T_{\mathrm{i}} \neq 0$, and $T_0 \approx T_1 \approx 0$. Also, if the condition of $g/N_{\mathrm{i}} \ll T_{\mathrm{i}} \ll N_{\mathrm{i}}$ is fulfilled, we can obtain $\rho_0 \approx g/T_{\mathrm{i}}$, $\gamma' \approx T_{\mathrm{i}} + 4.4\rho_0$, $\omega_{\mathrm{R}}^2 \approx 2g + 3.4\rho_0^2$, $\omega_{\mathrm{I}}^2 \approx kg/T_{\mathrm{i}}$, $f_0 \approx -gm$ and $f_1 = 0$.

Figure 2 shows the case of deep traps. R_1 reduces and Φ_1 deviates from 90° with the increase of the intensity I_{i}. This result suggests that using a low intensity we can improve the diffraction efficiency and

the coupling coefficient of two-wave coupling for deep traps. Figure 2(c) shows that the two response rates are all linear functions of I_i. This result agrees with that of the erasure process in Ref.[21].

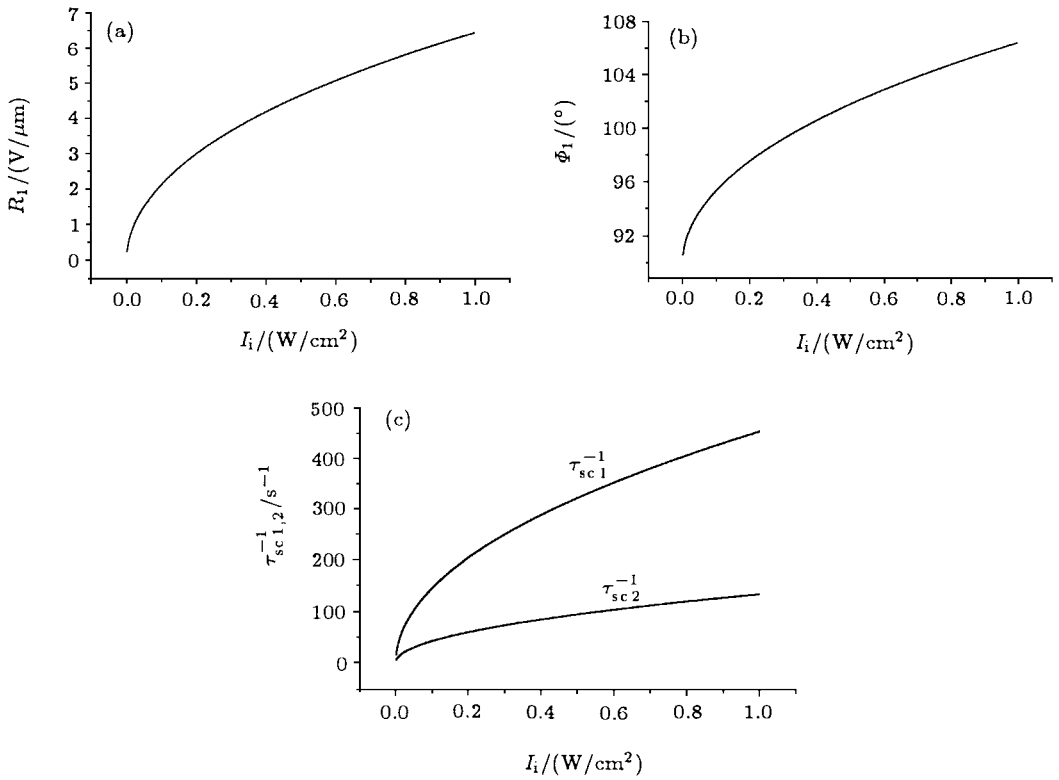


Fig.1. The relations between: (a) the amplitude of the steady-state SCF R_1 and the total incident intensity I_i; (b) the phase of the steady-state SCF Φ_1 and the total intensity I_i; (c) the two response rates and the total intensity I_i, at E_i=100V/μm and $k = 200$ for the case without traps.

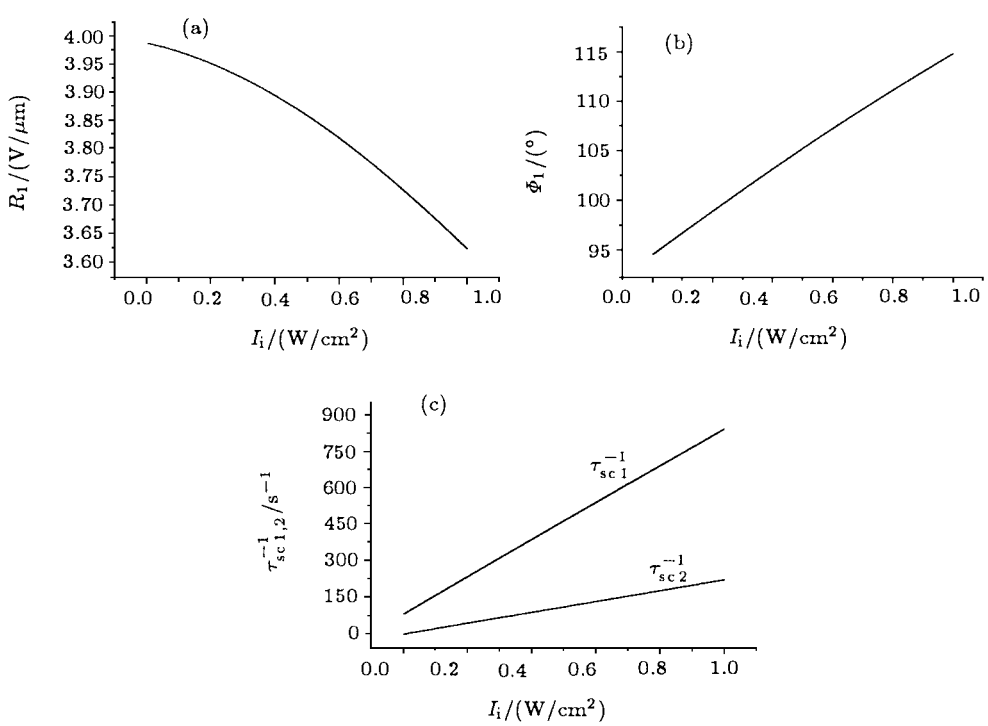


Fig.2. The relations between: (a) the amplitude of the steady-state SCF R_1 and the total intensity I_i; (b) the phase of the steady-state SCF Φ_1 and the total intensity I_i; (c) the two response rates and the total intensity I_i, at E_i=100V/μm, k=200 and T_i=8, for the case of deep traps.

3.1.3. Case with high-density traps

When the trap density is very high, even close to that of the initial acceptor density N_i, we could consider approximately $T_0 = T_\mathrm{i}$ and T_1=0 during the formation process of the SCF. Thus we have $\rho \approx g/T_\mathrm{i}$, $\gamma' \approx T_\mathrm{i}$, $\omega_\mathrm{R}^2 \approx 2g$, $\omega_\mathrm{I}^2 \approx kg(1/N_\mathrm{i} + 1/T_\mathrm{i})$, $f_0 \approx -gm$ and $f_1 = 0$. According to Eqs.(6) and (7) we notice that R_1 and Φ_1 are independent of I_i. Letting $T_\mathrm{i} = 1 \times 10^4$, we obtain $R_1 \approx 50\mathrm{V}/\mu\mathrm{m}$ and $\Phi_1 \approx 179.35°$. This means that we cannot have phase shift grating. Figure 3 shows that $\tau_{\mathrm{sc}\,1}^{-1}$ reduces weakly with the increase of I_i, and $\tau_{\mathrm{sc}\,2}^{-1}$ is a linear function of I_i. Actually, because $\tau_{\mathrm{sc}\,1}^{-1}$ is very large, we can completely neglect its effect, indicating that the formation of the SCF is in a single exponential form for the case of high-density traps.

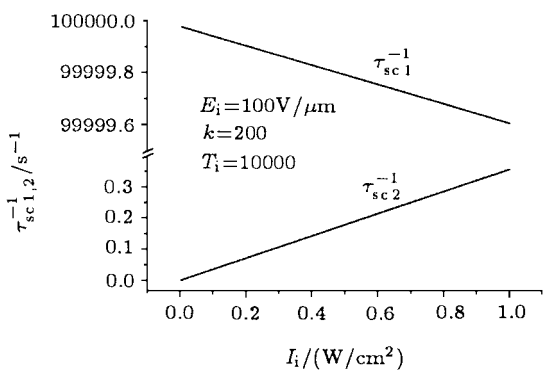


Fig.3. The relations between $\tau_{\mathrm{sc}\,1,2}^{-1}$ and the intensity I_i for the case of high-density traps.

3.2. Cases where f is a function of time

When we must consider the transient processes of trapping and detrapping, f becomes a function of time. The real form of the SCF can be expressed as

$$\begin{aligned} E(x,t) =& E_0 + \frac{E_1}{2}\exp(\mathrm{i}kx) + \frac{E_1^*}{2}\exp(-\mathrm{i}kx) \\ =& E_0 + R_1[\cos(kx + \Phi_1) - R_4 \\ & \times \exp(-t/\tau_\mathrm{T})\cos(kx + \Phi_1 + \Phi_1) - R_2 \\ & \times \exp(-t/\tau_{\mathrm{sc}\,1})\cos(kx + \Omega_1 t + \Phi_1 + \Phi_2) - R_3 \\ & \times \exp(-t/\tau_{\mathrm{sc}\,2})\cos(kx + \Omega_2 t + \Phi_1 + \Phi_3)], \end{aligned} \tag{10}$$

where R_2, R_3 and R_4 are the amplitudes of $\left[\frac{c_2}{c_2 - c_1}\left(1 - \Delta_1\frac{f_1}{f_0}\right)\right]$, $\left[\left(1 - \frac{c_2}{c_2 - c_1}\right)\left(1 - \Delta_2\frac{f_1}{f_0}\right)\right]$, and $\Delta_1\Delta_2\frac{-f_1}{f_0}$, respectively; and Φ_2, Φ_3 and Φ_4 are their phases, respectively. Other parameters are same as those in section 3.1.

According to the expressions of r_0, r_1, T_0, T_1, and Eq.(3), we give the coefficients

$$\rho_0 \approx \frac{\sqrt{g}}{2T_\mathrm{i}}[(4T_\mathrm{i}r_0 + g)(1 + 4g/T_\mathrm{i}^2)]^{1/2},$$

$$\gamma' \approx T_\mathrm{i} + 4.4\rho_0,$$

$$\omega_\mathrm{R}^2 \approx \rho_0(T_\mathrm{i} + 3.4\rho_0) + g,$$

$$\omega_\mathrm{I}^2 \approx k\rho_0,$$

$$f_0 \approx -gm - \frac{r_1 T_\mathrm{i}\rho_0(N_\mathrm{i}\rho_0 + g)}{N_\mathrm{i}(\rho_0 + r_0)^2},$$

$$f_1 \approx \frac{r_1 T_\mathrm{i}\rho_0(r_0 N_\mathrm{i} - g)}{N_\mathrm{i}(\rho_0 + r_0)^2},$$

where we take into consideration a condition of $r_1 + 1 \ll T_\mathrm{i} \ll N_\mathrm{i}$.

Figure 4 illustrates the relations between R_1, Φ_1 and the intensity I_i for k=25 and 200. Firstly, comparing Fig.4(a) with 4(c) and Fig.4(b) with 4(d), we know that the reducing grating vector k can improve R_1 and Φ_1. Secondly, we can see that, when the intensity is low, R_1 rises rapidly and then remains constant for high trap density T_i. But, in the case of low trap density T_i, R_1 reaches a maximum and then reduces with the enhancement of I_i, especially for a low grating wave vector k. Also, if k is low (such as k=25) R_1 can once more rise after it arrives at a minimum. These results have been experimentally found in inorganic PR crystals and can be explained by two types of carrier with multiple-trap-level models.[18] But we can directly obtain this from the basic equation. Φ_1 is also a function of the intensity I_i, the applied electric field E_i, the grating wave vector k, and the trap density T_i. For high trap density T_i, Φ_1 is nearer to 90° at low intensity than at high intensity. For low trap density T_i, Φ_1 is near to 90° at high intensity. Also, by reducing the trap density T_i we can observe a 90° phase shift.

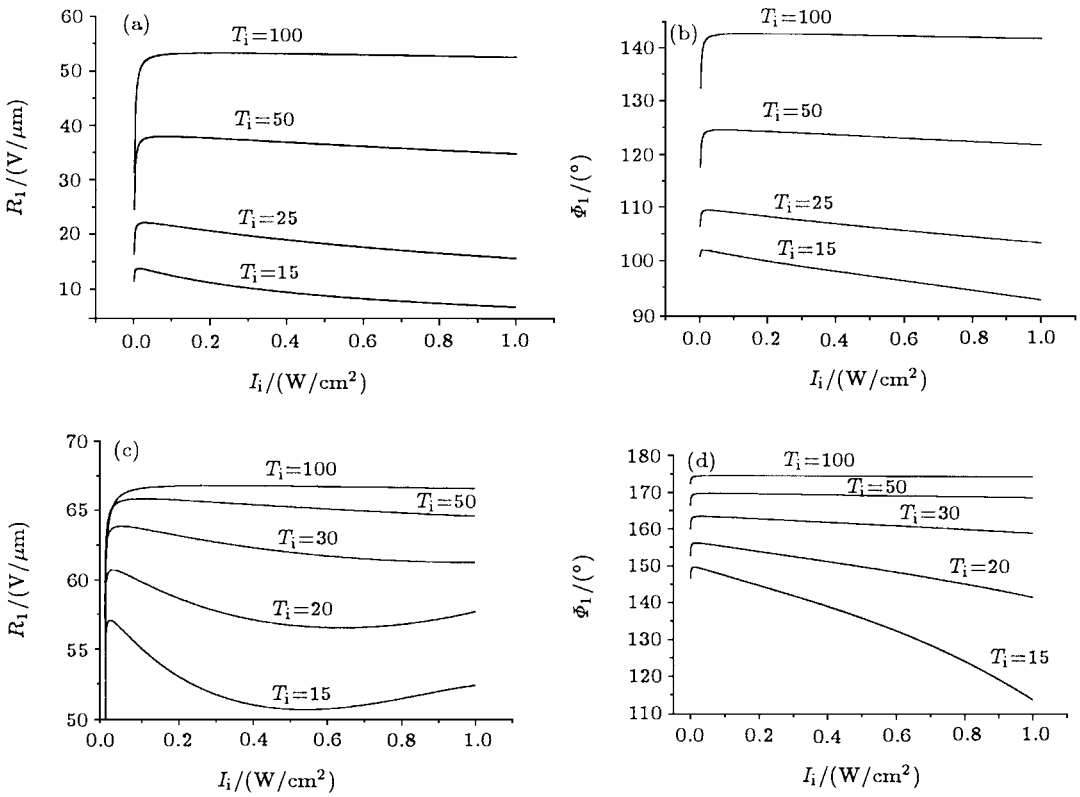


Fig.4. The relations for a general case of traps between: (a) the amplitude of the steady-state SCF R_1 and the total intensity I_i; (b) the phase of the steady-state SCF Φ_1 and the total intensity I_i, when E_i=100V/μm and k=200; (c) the amplitude of the steady-state SCF R_1 and the total intensity I_i; (d) the phase of the steady-state SCF Φ_1 and the total intensity I_i, when E_i=100V/μm and k=25.

Figure 5 plots the relations between the response rates and the intensity I_i. Firstly, by comparing Fig.5(a) with 5(c), we can see that whether k=25 or 200, $\tau_{sc\,1}^{-1}$ is always a superlinear function of I_i. But $\tau_{sc\,2}^{-1}$ is not the case. When k=25, it is a sublinear function of I_i and with the decrease of T_i it becomes a nonlinear function such as T_i=15, whereas if k=200, it is a superlinear function (see Figs.5(b) and 5(d)). In Ref.[21], both response rates are sublinear functions of the intensity I_i. This may be because of the different material parameters and the different applied electric fields E_i. In fact, if expressing these relations as $\tau_{sc\,1}^{-1} \propto I_i^{x_1}$, $\tau_{sc\,2}^{-1} \propto I_i^{x_2}$ and $\tau_T^{-1} \propto I_i^{x_3}$, then we have $x_1 > 1$, $x_2 > 1$ (when k is large) or $x_2 < 1$ (when k is small), and $x_3 > 1$. Next, from Fig.5 we find that increasing the trap density T_i can improve the fast response rate $\tau_{sc\,1}^{-1}$ and reduce the slow response rate $\tau_{sc\,2}^{-1}$ and τ_T^{-1}, implying that raising the trap density T_i can increase the difference between the fast and slow response rates. Figure 5(e) gives the curves of τ_T^{-1} versus I_i. Comparing the three response rates, we know that $\tau_{sc\,1}^{-1}$ is the fastest and τ_T^{-1} is near to $\tau_{sc\,2}^{-1}$.

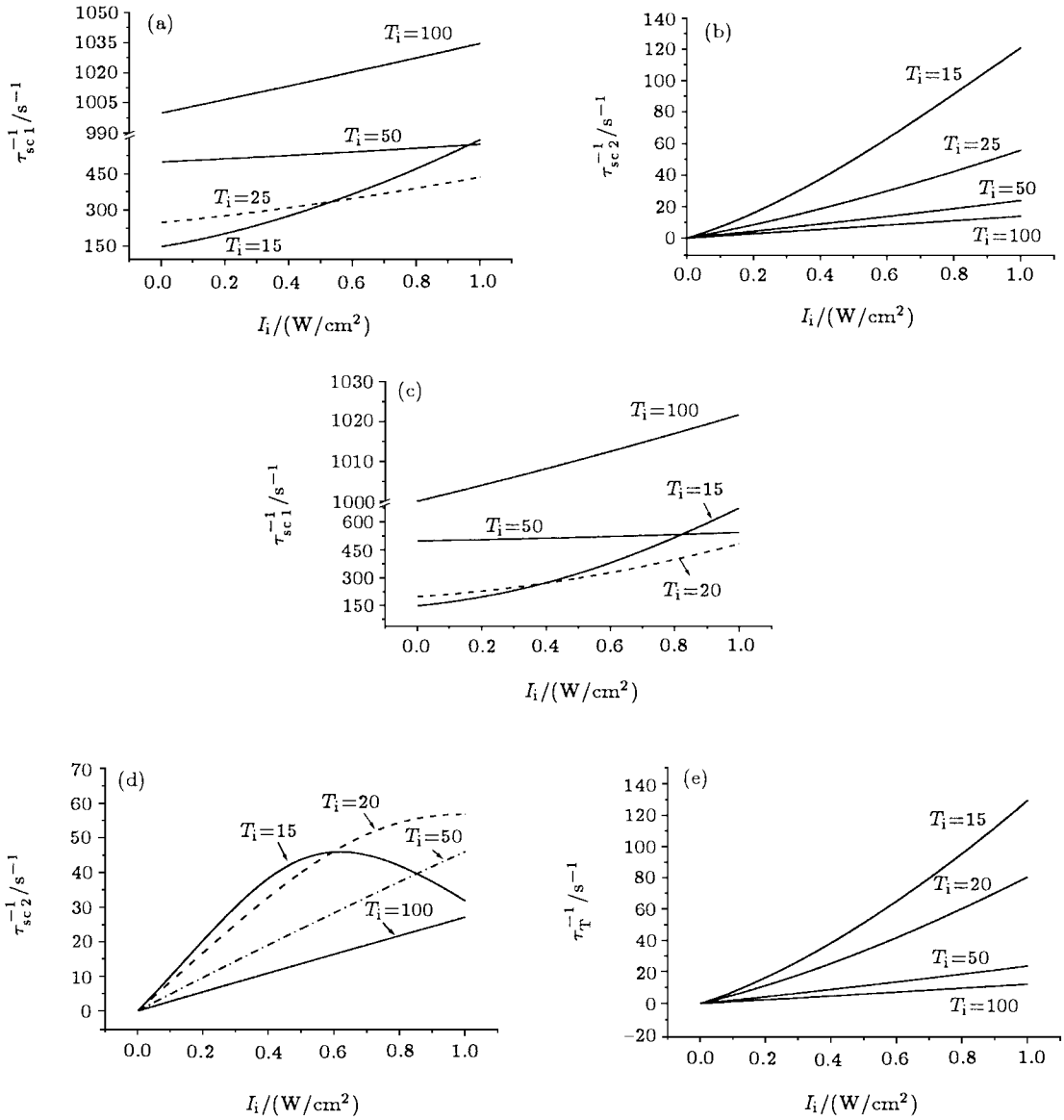


Fig.5. The relations for the general case of traps between the three response rates and the total intensity: (a) $\tau_{sc\,1}^{-1}$ versus I_i at E_i=100V/μm and k=200; (b) $\tau_{sc\,2}^{-1}$ versus I_i at E_i=100V/μm and k=200; (c) $\tau_{sc\,1}^{-1}$ versus I_i at E_i=100V/μm and k=25; (d) $\tau_{sc\,2}^{-1}$ versus I_i at E_i=100V/μm and k=25; (e) τ_T^{-1} versus I_i at E_i=100V/μm.

4. Experiments

The PR sample is a new composite, in which 40 wt% liquid crystal 4,4'-n-pentylcyanobiphenyl (5CB) as chromophores and 0.2 wt% C_{60} as a sensitizer are doped into the conductive polymer N-vinylcarbazole (PVK). This PR composite has been described in detail in Ref.[14]. The thickness of the sample is about 100μm and the glass transition temperature $T_g \approx 40^\circ$C. Using the usual wave-mixing method, we have measured the build-up processes of grating at an operated wave length of 632.8 nm. We have obtained the two response rates $\tau_{sc\,1,2}^{-1}$ through fitting the experimental data to the square of a bi-exponential function. The tilted angle of the sample normal with respect to the symmetric axis of the two writing beams was kept at 40°. The inner intersection angle of the two overlapped beams and the applied electric field were kept at 37° and 60V/μm, respectively. Four different total incident intensities were adopted: 0.859, 0.719, 0.557 and 0.468 W/cm^2. The ratio of the two writing beams was kept at 2:1. Figures 6 and 7 show the relations of the steady-state diffraction efficiency (η^{ss}) and the response rates ($\tau_{sc\,1,2}^{-1}$) with respect to the total incident intensity (I_i). It was found that η^{ss} decreases monotonically with the increase of the total incident intensity. This agrees with Fig.4(a) in the high-intensity region for the low trap density. In fact, the lowest-intensity irradiation

0.468 W/cm^2 in our experiment is still so high that we do not find the increase of η^{ss} with the intensity as the results in Fig.4(a) for the low-intensity region. However, many experimental results about the relations between η^{ss} and I_i in PRPs, reported by other researchers,[31] can confirm our theoretical results (Figs.6 and 7 in Ref.[31]). A superlinear relation between the response rate $\tau_{sc\,1}^{-1}$ and the total incident intensity is clearly seen in Fig.7(a). This agrees with the theoretical result in Fig.5(a) for low trap density. From Fig.7(b) we find that the response rate $\tau_{sc\,2}^{-1}$ increases linearly with the intensity for the first three intensity values. However, the response rate $\tau_{sc\,2}^{-1}$ rises rapidly for the fourth intensity value. We suppose that a superlinear relation between the response rate $\tau_{sc\,2}^{-1}$ and the intensity will occur if the intensity is further improved. So this result is in agreement with Fig.5(b) for the low trap density. Also, we can conclude that the samples PVK:5CB:C_{60} used in our experiments belong to the case of low trap density.

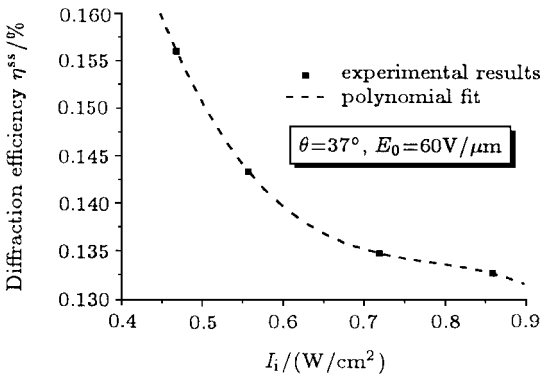


Fig.6. Experimental results of the relation between the steady-state diffraction efficiency η^{ss} and the total incident intensity I_i.

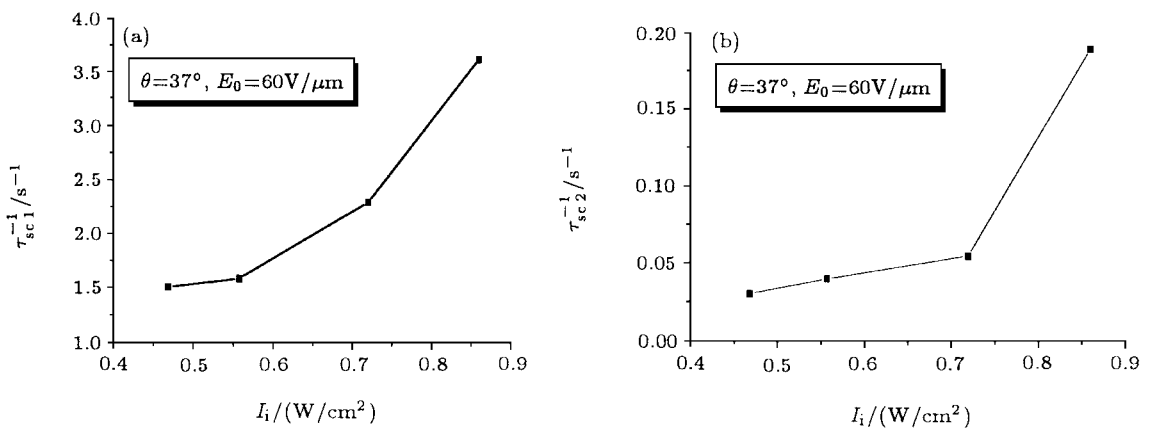


Fig.7. Experimental results of the relation between the response rates $\tau_{sc\,1,2}^{-1}$ and the total incident intensity I_i: (a) $\tau_{sc\,1}^{-1}$; (b) $\tau_{sc\,2}^{-1}$.

5. Conclusions

As mentioned in the introduction, the dependence of the space-charge field in photorefractive polymers on the total incident intensity have been studied and discussed. The results obtained show the following:

1. For the case without traps, $\tau_{sc\,1,2}^{-1} \propto I_i^{1/2}$. For the case with deep traps, $\tau_{sc\,1,2}^{-1} \propto I_i$. For the case with high-density traps, $\tau_{sc\,1}^{-1}$ is nearly a constant and $\tau_{sc\,2}^{-1} \propto I_i$. For the general case of traps, $\tau_{sc\,1}^{-1} \propto I_i^{x_1}$ ($x_1 > 1$) and $\tau_{sc\,2}^{-1} \propto I_i^{x_2}$ ($x_2 < 1$ for small grating vector k) or $\tau_{sc\,2}^{-1} \propto I_i^{x_2}$ ($x_2 > 1$ for large grating vector k). Also, with the increase of trap density T_i, both x_1 and x_2 become close to unity.

2. For the case without traps, the amplitude of the steady-state SCF increases monotonically with the total incident intensity. But, if the trap levels are deep and the density is not high, it reduces monotonically with the total incident intensity. For the case of high-density traps the steady-state SCF is independent of incident intensity. For the general case, with the rise of intensity it first increases and reaches a maximum, then either remains at the maximum for high trap density, or falls for low trap density.

3. In the intensity region of our experiments, the steady-state diffraction efficiency reduces with the total incident intensity. There is a superlinear relation between the response rate and the total incident intensity. The samples PVK:5CB:C_{60} used in our experiments belong to the case of low trap density.

All of the results suggest that the properties of static and temporal SCF are strongly dependent on the trap level and quantity.

References

[1] Ashkin A *et al* 1966 *Appl. Phys. Lett.* **9** 72
[2] Guo R *et al* 1997 *Acta Phys. Sin.* **46** 1681 (in Chinese)
[3] Günter P 1982 *Phys. Rep.* **93** 199
[4] Liu Y W *et al* 2000 *Acta Phys. Sin.* **49** 880 (in Chinese)
[5] Feng Y W *et al* 1998 *Acta Phys. Sin.* **47** 598 (in Chinese)
[6] Xu L *et al* 1998 *Acta Phys. Sin.* (*Overseas Edition*) **7** 283
[7] Zhao J L *et al* 2001 *Chin. Phys.* **10** 739
[8] Li Q *et al* 2000 *Chin. Phys.* **9** 841
[9] Ducharme S *et al* 1991 *Phys. Rev. Lett.* **66** 1846
[10] Donckers M C J M, Silence S M and Walsh C A 1993 *Opt. Lett.* **18** 1044
[11] Meerholz K *et al* 1994 *Nature* **371** 497
[12] Herlocker J A *et al* 1999 *Appl. Phys. Lett.* **74** 2253
[13] Cui Y *et al* 1997 *J. Phys. Chem.* B **101** 3530
[14] Zhang J and Singer K D 1998 *Appl. Phys. Lett.* **72** 2948
[15] Tayebati P and Mahgerefteh D 1991 *J. Opt. Soc. Am.* B **8** 1053
[16] Mahgerefteh D and Feinberg J 1990 *Phys. Rev. Lett.* **64** 2195
[17] Chang J Y *et al* 1995 *J. Opt. Soc. Am.* B **12** 248
[18] Li Y, Hou F, Liu S, Sun W and Xu K 1997 *Opt. Commum.* **134** 591
[19] Li Y, Liu S, Hong J and Xu K 1997 *J. Appl. Phys.* **81** 1752
[20] Valley G C 1986 *J. Appl. Phys.* **59** 3363
[21] Cui Y *et al* 1999 *J. Appl. Phys.* **85** 38
[22] Nishida F and Tomita Y 1997 *J. Appl. Phys.* **81** 3348
[23] Jones B E *et al* 1994 *J. Opt. Soc. Am.* B **11** 1064
[24] Shakos J D *et al* 1998 *Opt. Commum.* **150** 230
[25] Bäuml G, Schloter S and Hofmann U 1998 *Opt. Commum.* **154** 75
[26] Yuan B, Sun X, Hou C, Li Y, Zhou Z, Jiang Y and Li C 2000 *J. Appl. Phys.* **88** 5562
[27] Yuan B, Sun X, Jiang Y, Hou C and Zhou Z 2001 *J. Mod. Opt.* 48 1161
[28] Twarowski A 1989 *J. Appl. Phys.* **65** 2833
[29] Schildkraut J S and Buettner A V 1992 *J. Appl. Phys.* **72** 1888
[30] Schildkraut J S and Cui Y 1992 *J. Appl. Phys.* **72** 5055
[31] Wang L M, Ng M K and Yu L P 2000 *Phys. Rev.* B **62** 4973